Macrocyclization of Peptide Side Chains by the Ugi Reaction: Achieving Peptide Folding and Exocyclic *N*-Functionalization in One Shot

Aldrin V. Vasco,[†,‡] Carlos S. Pérez,[†] Fidel E. Morales,[†] Hilda E. Garay,[§] Dimitar Vasilev,[⊥] José A. Gavín,[‖] Ludger A. Wessjohann,*[,⊥] and Daniel G. Rivera*[,†]

[†]Center for Natural Products Research, Faculty of Chemistry, University of Havana, Zapata y G, 10400, La Habana, Cuba

[‡]Facultad de Ingeniería Química, Instituto Superior Politécnico José Antonio Echeverría, CUJAE, Calle 114 # 11901, 11500, La Habana, Cuba
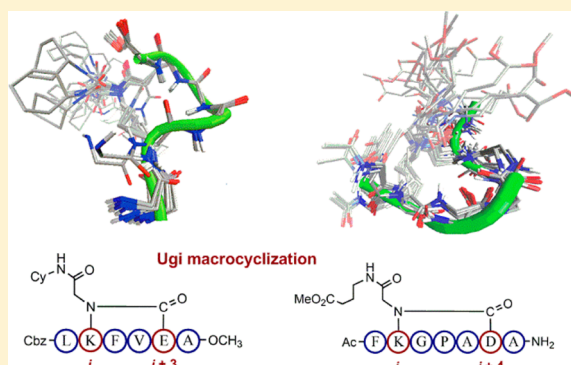
[§]Synthetic Peptides Group, Center for Genetic Engineering and Biotechnology, P.O. Box 6162, La Habana, Cuba

[‖]Instituto Universitario de Bioorgánica Antonio González and Departamento de Química Orgánica, Universidad de La Laguna, 38206 La Laguna, Tenerife, Spain

[⊥]Department of Bioorganic Chemistry, Leibniz Institute of Plant Biochemistry, Weinberg 3, D-06120, Halle/Saale, Germany

S *Supporting Information*

ABSTRACT: The cyclization of peptide side chains has been traditionally used to either induce or stabilize secondary structures (β-strands, helices, reverse turns) in short peptide sequences. So far, classic peptide coupling, nucleophilic substitution, olefin metathesis, and click reactions have been the methods of choice to fold synthetic peptides by means of macrocyclization. This article describes the utilization of the Ugi reaction for the side chain-to-side chain and side chain-to-termini macrocyclization of peptides, thus enabling not only access to stable folded structures but also the incorporation of exocyclic functionalities as *N*-substituents. Analysis of the NMR-derived structures revealed the formation of helical turns, β-bulges, and α-turns in cyclic peptides cross-linked at i, $i + 3$ and i, $i + 4$ positions, proving the folding effect of the multicomponent Ugi macrocyclization. Molecular dynamics simulation provided further insights on the stability and molecular motion of the side chain cross-linked peptides.

INTRODUCTION

Constraining short peptides into protein-like bioactive conformations remains as a synthetic challenge with growing implications in the development of peptide-based therapeutic agents.[1] Cyclization[2,3] and conjugation to topological templates[4] are the most successful methods to introduce conformational constraints in peptides designed either as protein ligands or mimetics of protein epitopes. However, cyclization stands as the most effective, and consequently employed, way to access folded peptide sequences mimicking biologically relevant secondary structures (i.e., β-hairpins, β-strands, α-helix, and turns).[3] In addition, cyclic peptides usually exhibit an enhanced binding affinity to the biological target[5] as well as improved pharmacological properties compared to their acyclic analogues.[6] Consequently, there has been a resurgence of chemical[2,6] and enzymatic[7] approaches aiming at the efficient cyclization of peptides either by their termini or side chains.

While head-to-tail and side chain-to-main chain cyclizations are of wide incidence in natural nonribosomal peptides, the disulfide bridge is nature's solution for the structural

preorganization of peptides and proteins by means of side chain-to-side chain linkage. Synthetic chemists have developed a variety of side chain-to-side chain cyclization methods to constrain peptides to strand, helix, turn, and loop conformations.[2,3] Such approaches include the lactam bridge formation between the side chains of Lys and Asp/Glu residues,[8] the Cu[I]-catalyzed alkyne—azide 1,3-dipolar cycloaddition,[9] olefin metathesis,[10] nucleophilic substitution,[11] and aryl—aryl coupling,[12] among others.

In the last years, isocyanide-based multicomponent reactions (I-MCRs) have emerged as powerful macrocyclization procedures enabling the rapid access to new macrocyclic chemotypes,[13] including *pseudo*-peptidic ones.[14] In particular, the Ugi four-component reaction was the first one being employed for the head-to-tail cyclization of peptides as far as in 1979.[15] However, the interest in utilizing this reaction for peptide cyclization dropped over the following 30 years,[13b]
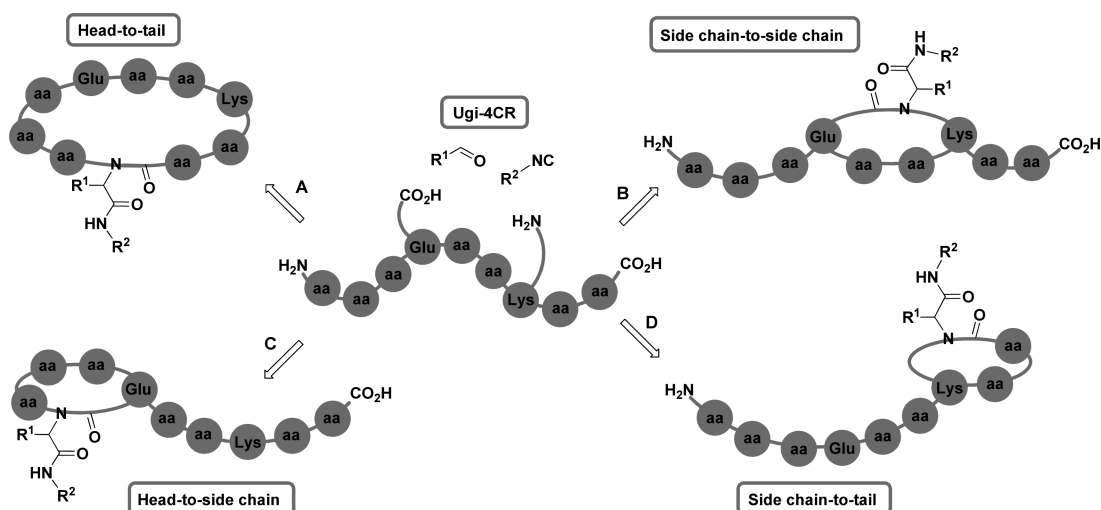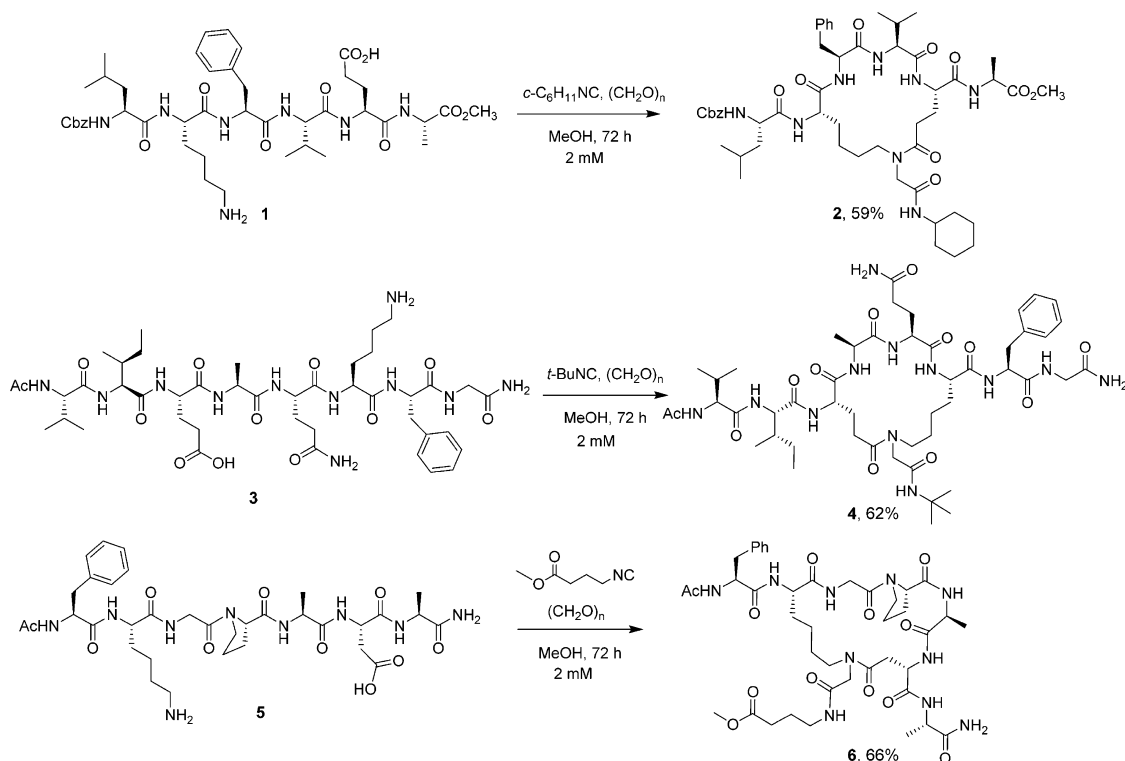
Figure 1. Peptide macrocyclization strategy using the Ugi reaction.

Scheme 1. Side Chain-to-Side Chain Peptide Macrocyclizations by the Ugi Reaction

mainly because of the longer reaction times and lower yields compared to the classic peptide coupling protocols. Despite the drawbacks related to the Ugi cyclization by the peptide termini, there are other synthetic options involving the utilization of peptide side chains that may lack such problems, and yet remain unexplored.

Figure 1 illustrates the four possibilities of peptide macrocyclization by means of the Ugi reaction, including the head-to-tail cyclization (A) previously reported.[15] As this reaction is the condensation of an amino and a carboxylic group with an oxo component and an isocyanide, cyclization strategies B, C, and D rely on the presence of Glu/Asp and Lys/Orn along the peptide sequence. Perhaps the most important feature of this strategy—and the one that distinguishes it more from the

classic peptide coupling—is the generation of an exocyclic functionality as part of the N-substituted amide formed during the ring closing step. We envisioned that the exploitation of such a characteristic may provide a variety of applications not so easily available for conventional cyclization methods based on coupling reagents.

Herein we demonstrate that the Ugi-4CR is a suitable procedure for the macrocyclization of peptide side chains, thus leading to cyclic peptides bearing a tertiary lactam bridge instead of a secondary one, i.e., N-substituted cyclic peptides. Our aim is to prove the potential of this approach to fulfill two objectives in only one synthetic operation, i.e., the incorporation of an exocyclic functionality as part of the N-alkylation and the introduction of conformational constraints leading to

folded peptides. To get deep insights into the three-dimensional structures of the *N*-substituted cyclic peptides in solution, a molecular modeling study based on NMR restraints and molecular dynamics was performed.

■ RESULTS AND DISCUSSION

Macrocyclization of Peptide Side Chains by the Ugi Reaction. Several reports have shown the scope and limitations of the Ugi reaction in the macrocyclization of dissimilar substrates,[16] including peptidic ones.[17,18] According to the mechanism of the Ugi reaction (Figure 1B)—in which the initially formed α-adduct evolves through an intramolecular acylation (Mumm rearrangement) to the final product—the migration capacity of the amino component is crucial on the reaction length and efficiency. In this sense, Yudin et al. have proposed that the slow kinetics of the Ugi macrocyclization in short peptides is due to the slow transannular attack of the amine to the mixed anhydride.[19] As an alternative to the conventional Ugi reaction, Yudin's group introduced the use of an amphoteric aziridine aldehyde in a new multicomponent peptide macrocyclization deviating from the Mumm rearrangement.[19] Such a modified Ugi macrocyclization allowed the efficient and highly stereoselective head-to-tail cyclization of short- and medium-size peptides.[19,20] In contrast to linear peptides, small pentapeptoids (i.e., *N*-alkylated pentaglycines) have been successfully cyclized by the Ugi reaction,[17] confirming that a greater flexibility of the amine moiety facilitates the macrocyclic Ugi-based ring closure.

Recently, we described the development of a bidirectional macrocyclization strategy based on the execution of two Ugi reactions between peptide diacids and diisocyanide cross-linkers.[18] In that study, macrocyclizations based on side chain carboxylic groups were much more efficient than those relying on the more conformationally constrained backbone carboxylic groups. In a similar way, we anticipated that unidirectional Ugi macrocyclizations using the flexible Glu/Asp and Lys side chains would be less problematic than the head-to-tail version, as they may skip the difficulties associated with the slow Mumm rearrangement.

Scheme 1 depicts three examples of side chain-to-side chain peptide macrocyclization by means of the Ugi reaction between Glu/Asp and Lys side chains. Our aim lies at utilizing the cyclization to fold peptide scaffolds onto turn structures, while introducing a *N*-substitution as an exocyclic functionality. As mentioned above, several peptide cyclization methods have been employed to stabilize turns,[3] though none of them allows for the simultaneous exocyclic *N*-functionalization of the cyclization site. The potential of accomplishing cyclization and *N*-substitution in one step is remarkable, as three crucial goals can be achieved in one shot: (a) improving pharmacological properties through the *N*-alkylation,[21] (b) accessing specific secondary structures of biological relevance, and (c) employing the resulting exocyclic *N*-functionality, e.g., for conjugation/immobilization strategies.
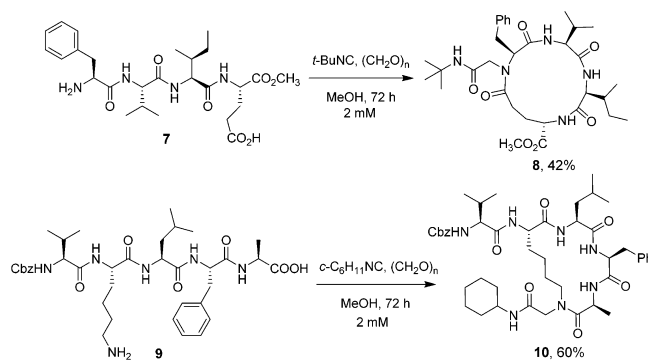
As shown in Scheme 1, three different oligopeptides were subjected to side chain-to-side chain Ugi macrocyclization in solution. Such linear peptides were produced either by a stepwise solution-phase synthesis or by a standard Fmoc solid-phase protocol.[22] The strategy was the introduction of amino acids with Ugi-reactive side chains located at *i*, *i* + 3 and *i*, *i* + 4 positions, as these combinations are known to stabilize both turns and helical structures.[3a,23] Thus, peptides **1** and **3** bear the Lys/Glu and Glu/Lys pairs located at the *i* and *i* + 3 positions

running from the *N*- to *C*-terminus direction, while peptide **5** has the Lys and Asp residues located at *i* and *i* + 4 positions. It must be noticed that amino acid sequences were not designed to favor a periodic secondary structure (e.g., α-helix and β-sheet), but the goal is to assess the effect of the Ugi macrocyclization on the peptide folding.

Macrocyclizations were carried out in methanol at 2 mM concentration, always using paraformaldehyde as the oxo component in order to form only one diastereomer. Besides using commercially available isocyanides, synthesis of cyclic peptide **6** demonstrates the possibility of incorporating an exocyclic reactive functionality suitable for further derivatization. In all cases, preformation of the imine was initially accomplished at higher concentration (10 mM), followed by dilution to the final concentration and addition of the isocyanide. HPLC monitoring of Ugi macrocyclization affording **2** proved high conversion (≥80%) after 72 h of reaction. Thus, the general reaction time was fixed to 72 h for all macrocyclizations to enable comparison of efficiency among the different approaches. Cyclic peptides **2**, **4**, and **6** were obtained in good yield (ca. 60%) and high purity (>95%) after preparative HPLC purification, which renders enough material for assessing the solution three-dimensional structure through NMR analysis.

To expand the scope of the Ugi macrocyclization, we sought to assess the efficacy of this method for tethering peptide side chains to each one of the termini, thus showing the two remaining Ugi-cyclizing combinations. Scheme 2 depicts the
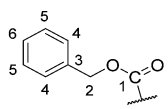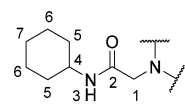
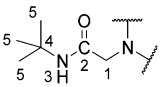**Scheme 2. Side Chain-to-Termini Peptide Macrocyclizations by the Ugi Reaction**

implementation of head-to-side chain and side chain-to-tail macrocyclizations leading to peptides **8** and **10**, respectively. As shown, tetra- and pentapeptides were cyclized by side chains of amino acids separated two residues from one of the termini. Interestingly, the yield of isolated cyclic peptide **8** was the lowest among all macrocyclizations, but there were no great differences between the procedure yielding **10** and those giving, for example, **2** and **4**. It must be noticed that the more efficient Ugi macrocyclizations are those employing the amino group of the flexible Lys side chain, despite the fact that macrocycles **2**, **4**, **6**, and **10** feature different ring sizes. Alternatively, Ugi macrocyclization to cyclic peptide **8** comprises the reaction of a backbone terminal amino group, which seems to share with the head-to-tail approach the mechanistic complications derived from a slow transannular acylation. Two additional cyclizations (not shown) featuring the same head-to-Glu side chain cyclization, but with different tetrapeptide sequences, were also studied. In those cases, HPLC/ESI-MS monitoring showed

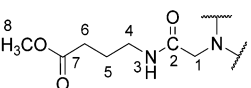**Table 1. ^{1}H NMR Assignment of Cyclic Peptides 2, 4, and 6**

			Cyclic peptide 2		
Residue	NH (m, J (Hz))	H$^\alpha$	H$^\beta$	H$^\gamma$	Others
Leu	7.36 (d, 8.0)	4.02	1.20, 1.38	1.56	0.81 , 0.85 (2×CH$_3\delta$)
Lys	7.87 (d, 8.2)	4.30	1.69, 1.42	1.25, 1.35	1.52, 1.41 (Hδ); 2.90, 3.45 (Hϵ)
Phe	8.73 (d, 8.9)	4.42	2.77, 3.15	-	7.17 (Hδ); 7.20 (Hϵ) ; 7.13 (Hζ)
Val	6.72 (d, 8.7)	4.30	2.00	0.83, 0.90	-
Glu	8.32 (d, 9.1)	4.30	1.57, 2.21	2.35, 2.40	-
Ala	8.23 (d, 3.9)	4.03	1.21	-	3.64 (OCH$_3$)

Cbz group

5.01 (H2); 7.34 (H4); 7.35 (H5); 7.30 (H6)

Exocyclic *N*-substituent produced by cyclization

3.72, 3.90 (H1); 7.54 (H3, J=7.8 Hz); 3.50 (H4); 1.65, 1.63, 1.21, 1.11, 1.19, 1.17, 1.15 (not assigned)

			Cyclic peptide 4		
Residue	NH (m, J (Hz))	H$^\alpha$	H$^\beta$	H$^\gamma$	Others
Val	7.92 (d, 9.0)	4.18	1.93	0.79; 0.81	1.85 (acetyl CH$_3$)
Ile	7.84 (d, 8.8)	4.15	1.69	1.41,1.05 (CH$_2$); 0.79 (CH$_3$)	0.79 (CH$_3$ δ)
Glu	7.96 (d, 7.1)	4.26	1.75, 1.84	2.26, 2.61	-
Ala	8.15 (d, 6.4)	4.07	1.26	-	-
Gln	7.82 (d, 6.7)	4.02	1.76	2.07	7.31; 6.80 (NH$_2$)
Lys	7.94 (d, 9.4)	4.25	1.55, 1.35	1.16	1.48, 1.36 (Hδ); 3.21 (Hϵ)
Phe	8.03 (d, 8.1)	4.49	3.03, 2.80	-	7.22 (Hδ); 7.24 (Hϵ); 7.17 (Hζ)
Gly	8.31 (t, 6.0)	3.56, 3.65	-	-	7.18, 7.08 (terminal CONH$_2$)

Exocyclic *N*-substituent produced by cyclization

3.70, 3.85 (H1); 7.40 (H3); 1.23 (H4)

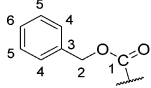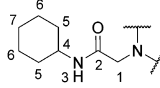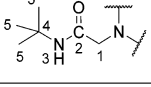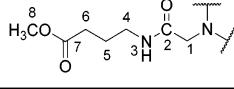|			Cyclic peptide 6		
Residue	NH (m, J (Hz))	H$^\alpha$	H$^\beta$	H$^\gamma$	Others
Phe	8.03 (d, 8.5)	4.52	2.93, 2.68	-	7.23 (Hδ); 7.25 (Hϵ); 7.18 (Hζ) 1.73 (acetyl CH$_3$)
Lys	8.05 (d, 8.4)	4.34	1.68, 1.44	1.30	1.69, 1.42 (Hδ); 3.06, 3.42 (Hϵ)
Gly	8.44 (m)	4.38, 3.72	-	-	-
Pro	-	4.16	2.19, 1.82	1.93; 1.89	3.73; 3.51 (δ)
Ala I	8.24 (d, 6.3)	4.14	1.30	-	-
Asp	7.53 (d, 7.6)	4.59	3.12, 2.54	-	-
Ala II	7.60 (d, 7.5)	4.09	1.23	-	7.01; 7.04 (terminal CONH$_2$)

Exocyclic *N*-substituent produced by cyclization

4.08, 3.60 (H1); 7.65 (H3); 3.11, 3.02 (H4); 1.63 (H5); 2.20 (H6); 3.58 (H8)

conversion no greater than 50% after 72 h, confirming the difficulties associated with the Ugi macrocyclization of short peptides utilizing the *N*-terminus as the amino component. So far, we can summarize that the Ugi reaction is an effective method for side chain-to-side chain and side chain-to-tail cyclizations, enabling a straightforward access to macrocyclic peptides bearing an exocyclic *N*-substitution. Albeit yields seem to be lower than those of peptide side chain cyclization with coupling agents, it must be considered that four covalent bonds are formed in the multicomponent reaction, while only one is formed in the peptide coupling.

Three-Dimensional Structure of Side Chain-to-Side Chain Cross-Linked Peptides. To assess the effect of the Ugi macrocyclization on the three-dimensional solution-phase structures of the side chain cross-linked peptides, we chose compounds 2, 4, and 6 to be studied by means of NMR and

Table 2. ^{13}C NMR Assignment for Cyclic Peptides 2, 4, and 6

				Cyclic peptide 2	
Residue	CO	C$^{\alpha}$	C$^{\beta}$	C$^{\gamma}$	Others
Leu	171.8	52.9	40.9	24.2	21.3; 23.2 (2×CH$_3$ δ)
Lys	171.4	52.4	32. 9	22.6	28.1 (Cδ), 48.4 (Cε)
Phe	170.2	54.3	37.3	137.9	128.8 (Cδ); 128.2 (Cε), 126.2 (Cζ)
Val	172.4	56.0	31.4	17.4; 19.2	-
Glu	170.4	50.5	27.1	27.7	171.4 (Cε)
Ala	172.5	49.0	17.0	-	52.0 (OCH$_3$)

Cbz group

155.9 (C1); 65.3 (C2); 137,2 (C3); 127.6 (C4); 128.4 (C5); 127.8 (C6)

Exocyclic *N*-substituent produced by cyclization

48.7 (C1); 167.3 (C2); 47.5 (C4); 32.3; 32.4; 25.2; 24.7; 24.7 (not assigned)

				Cyclic peptide 4	
Residue	CO	C$^{\alpha}$	C$^{\beta}$	C$^{\gamma}$	Others
Val	171.1	57.7	30.4	18.2; 19.3	22.5 (acetyl CH$_3$); 165.9 (acetyl CO)
Ile	170.4	56.7	36.6	24.4 (CH$_2$); 15.2 (CH$_3$)	11.07 (Cδ)
Glu	170.3	51.9	27.7	28.3	171.8 (Cδ)
Ala	171.9	48.9	17.8	-	-
Gln	171.2	53.1	27.1	31.3	173.8 (Cδ)
Lys	171.7	51.7	31.9	21.9	27.4 (Cδ); 47.9 (Cε)
Phe	171.3	54.0	37.4	137.6	129.2 (Cδ); 128.1 (Cε); 126.3 (Cζ)
Gly	170.7	41.9	-	-	-

Exocyclic *N*-substituent produced by cyclization

47.5 (C1); 167.7 (C2); 50.1 (C4); 28.6 (C5)

				Cyclic peptide 6	
Residue	NH (m, *J* (Hz))	H$^{\alpha}$	H$^{\beta}$	H$^{\gamma}$	Others
Phe	171.0	53.8	37.7	138.0	129.2 (Cδ); 128.0 (Cε); 126.2 (Cζ); 169.1 (acetyl CO); 22.5 (acetyl CH$_3$)
Lys	171.6	52.1	31.5	22.2	27.4 (Cδ) ; 48.6(Cε)
Gly	169.6	41.1	-	-	-
Pro	172.7	61.4	29.1	24.5	46.6 (Cδ)
Ala I	172.6	49.7	16.2	-	-
Asp	170.9	50.6	34.0	170.4	-
Ala II	173.8	48.4	17.9	-	-

Exocyclic *N*-substituent produced by cyclization

48.5 (C1); 168.0 (C2); 38.0 (C4); 24.4 (C5); 30.1 (C6); 173.2 (C7); 51.3 (C8)

molecular dynamics simulation. Similarly to other Lys-Asp/Glu cross-linked peptides made by classic lactamization, it is likely that the Ugi macrocyclization not only introduces significant conformational constraints onto small peptides but also leads to folded structures.[3a] Due to low solubility in water, structural characterization was accomplished on the basis of 1D and 2D ^{1}H NMR spectroscopy in DMSO-d_6 at 300 K. Full NMR assignment of these compounds is reported in Tables 1 and 2. Final structures were derived from coupling constants ($^3J_{NHCH\alpha}$) and ROE constraints and obtained by simulated annealing and refinement protocols in Xplor-NIH.[24]

We expected that cyclic peptides **2** and **4**—cross-linked with Lys and Glu separated by two residues—might have a C$^{\alpha}_{i}$–C$^{\alpha}_{i+3}$ distance lower than 7 Å, typical of reverse and helical turns. For cyclic peptide **2**, coupling constants $^3J_{NHCH\alpha}$ were higher than 8 Hz for all residues, except for C-terminal Ala (see the Supporting Information). Such values are indicative of a well-structured peptide skeleton of low conformational freedom, and are commonly associated with β-strand structures. Intriguingly, only three signals were observed in the C$^{\alpha}$H region of the ^{1}H NMR spectrum. The HSQC-edit spectrum of **2** (Figure 2) shows an overlapping of Hα resonances of Lys2, Val4, and Glu5 at 4.30 ppm, which makes impossible the unequivocal assignment of ROE cross-peaks involving these hydrogens and, consequently, its use as an experimental constraint in structure refinement. A total of 37 distance
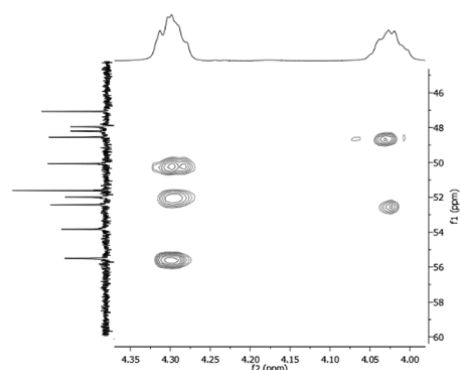
Figure 2. Expanded $C^\alpha H$ region of the HSQC-edit spectrum of peptide **2**.

constraints (5 strong, 18 medium, and 14 weak; 22 inter-residual: 10 of them sequential and 12 nonsequential) resulted from analysis of ROE intensities. Six dihedral restraints were used in the MD simulation, five ϕ angles from the $^3J_{NHCH\alpha}$ data and one χ_1 angle from the Phe residue. After three rounds of simulation, we could stereospecifically assign the methylene hydrogens of Phe3, the Hε of Lys3, and methyl groups of Val4.

Figure 3A (top) depicts the superimposition of the 20 lowest energy structures of cyclic peptide **2**, featuring 0.14 Å average RMSD to the mean structure for the peptide backbone that confirms the great conformational rigidity suggested by the $^3J_{NHCH\alpha}$ values. As shown, the NMR-derived solution structures of **2** comprise a reverse turn with propensity to helicity; i.e., the ϕ and ψ angles of Phe3, Val4, and Glu5 lay within the helical region. To determine whether such a behavior remains in time, we performed a further MD simulation during 80 ns from the average NMR-derived structure. Figures 3B (top) shows the ϕ/ψ distribution in time of the four central amino acids obtained from MD, confirming that the most populated states are confined to the helical space of Ramachandran plots. Also shown are three of the most representative structures obtained during simulation time, which show that the greater mobility lies at the first two residues Leu1 and Lys2. This comprises that the two N-terminal residues may pass through a *pseudo*-planar conformation, while residues Phe3, Val4, and Glu5 mostly remain in a helical conformation. In addition, various relevant hydrogen bonds were detected during MD simulation, including $CO_{Lys2}\cdots NH_{Ala6}$ (6% in time; $i, i + 4$ characteristic of α-helix), $CO_{Lys2}\cdots NH_{Glu5}$ (2% in time), and $CO_{Phe3}\cdots NH_{Ala6}$ (3% in time).

Cyclic peptide **4** also contains a N-substituted lactam bridge of Glu and Lys side chains at i and $i + 3$ positions but with the opposed directionality with respect to peptide **2**. Previously, it has been reported that the position of the amide group in the linker is crucial for stabilization of helical structures in peptide cross-linked at $i, i + 4$ positions.[8e] As a result, we sought to evaluate whether the change in the amide position might be important also in the folding of peptides cross-linked at $i, i + 3$.
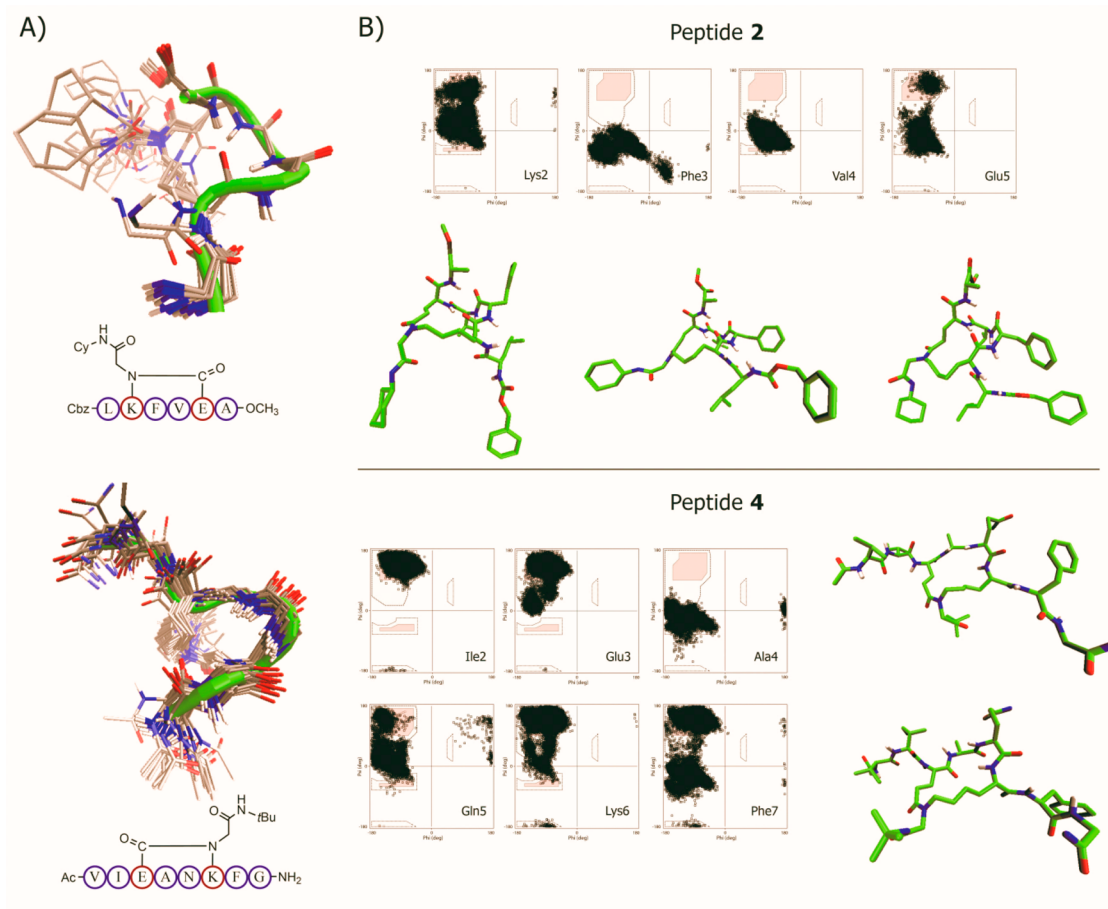

Figure 3. (A) Superimposition of 20 lowest energy structures of cyclic peptides **2** and **4**. (B) Distribution in time of ϕ and ψ angles (Ramachandran plots) for central amino acids of peptides **2** and **4**, and some representative structures as obtained from MD simulation.

For peptide **4**, $^3J_{\text{NHCH}\alpha}$ coupling constants of residues Val1, Ile2, Lys6, and Phe7 were >8 Hz, while $^3J_{\text{NHCH}\alpha}$ values of central residues Glu3, Ala4, and Gln5 were between 6 and 7 Hz. Analysis of the ROESY spectrum of **4** resulted in a total of 43 distance constraints (13 strong, 16 medium, and 14 weak; 28 inter-residual: 22 of them sequential and only 6 non-sequential). An important characteristic is the abundance of intense $d_{\alpha\text{N}}(i, i + 1)$ ROEs, which is indicative of β-sheet structures, but the lack of long-range $d_{\alpha\text{N}}(i, j)$ and $d_{\text{NN}}(i, j)$ ROEs. Along with the high $^3J_{\text{NHCH}\alpha}$ values of residues Val1, Ile2, Lys6, and Phe7, ROESY-derived information suggests β-strand conformations for sequences flanking the central amino acids Ala4 and Gln5. During molecular modeling, five dihedral restraints from $^3J_{\text{NHCH}\alpha}$ coupling constants were considered. The stereospecific assignment of relevant methylene hydrogens was possible after three rounds of simulation. Figure 3A (bottom) depicts the superimposition of the final 20 lowest energy structures of **4** (0.68 Å RMSD difference to the mean structure for the backbone), which comprise a β-strand with a change in the directionality due to the presence of a reverse turn at the central residues. Further MD analysis carried out during 80 ns of simulation revealed that the reverse turn transits from a tighter (only 17% in time) to a looser disposition (most populated), as shown in the two representative conformations illustrated in Figure 3B (bottom). MD simulation also confirmed that the average distance $C^{\alpha}_{\text{Glu3}}–C^{\alpha}_{\text{Lys6}}$ is around 7 Å (6.77 ± 0.51 Å). In the looser conformations of the central turn of peptide **4**, the irregularity in the β-strand chain caused by residues Ala4 and Gln5 resembles a β-bulge, i.e., a protuberance that affects the directionality of β-strands but in a less drastic manner than β-turns.[25] This is supported by the fact that φ and ψ angles of residue Ala4 lay within the right-handed helical region of the Ramachandran plot, while the remaining residues mostly populate the β-sheet space (Figure 3B), which is a common characteristic of classic β-bulges.[25]

Combined NMR/MD analysis was also performed for peptide **6**, which is cross-linked at i, i + 4 residues by a N-substituted lactam bridge. Previously, it has been reported that lactamization of Lys and Asp residues located at i, i + 4 positions is a very effective way to stabilize an α-helix in small peptides.[8a] In our case, we chose to introduce the turn-inducing amino acids Pro and Gly at the middle of the peptide sequence instead of using other sequences favoring helicity (e.g., poly-Ala or poly-Leu). Accordingly, we anticipated that cyclic peptide **6** could fold onto a *pseudo*-planar α-turn rather than in a α-helical conformation.

For peptide **6**, $^3J_{\text{NHCH}\alpha}$ coupling constants higher than 8 Hz were only found for residues Phe1 and Lys2, while $^3J_{\text{NHCH}\alpha}$ values of the remaining residues were between 6 and 8 Hz. As a result, there is no clear inclination either to helical or to β-strand structures. A total of 42 distance constraints (6 strong, 7 medium, and 29 weak; 19 inter-residual: 16 of them sequential and only 3 nonsequential) resulted from the ROESY spectrum. As most inter-residual ROE contacts were between sequential amino acids, this evidence indicates low propensity to either helical or tight turn conformations.

Figure 4A shows the superimposition of the 20 lowest energy NMR-derived structures of **6** (0.86 Å RMSD difference to the mean structure for the backbone), illustrating that this peptide occurs in a rather loose reverse turn including five residues (α-turn). Analysis of the distance $C^{\alpha}_{\text{Lys2}}–C^{\alpha}_{\text{Asp6}}$ reveals that, in 15 of the 20 lowest energy structures, the value is lower than 7 Å,
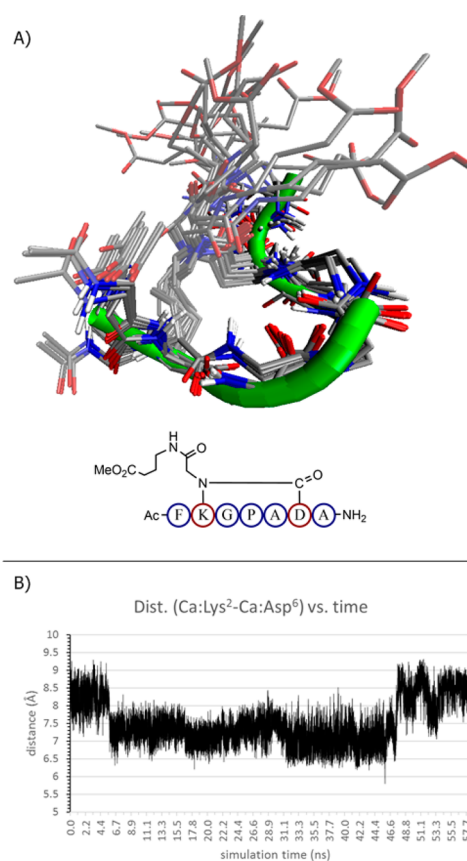

Figure 4. (A) Superimposition of 20 lowest energy structures of cyclic peptide **6**. (B) Plot of $C^{\alpha}_{\text{Lys2}}–C^{\alpha}_{\text{Asp6}}$ distance vs time as obtained from MD simulation.

while five structures had a distance greater than 7 Å. To get deeper insight into the loose character of the α-turn, we performed a MD simulation during 60 ns starting from the NMR-derived lowest energy structure. Figure 4B depicts the plot of $C^{\alpha}_{\text{Lys2}}–C^{\alpha}_{\text{Asp6}}$ distances versus time, indicating that such distances vary from 6.5 to around 9 Å. However, most populated states lay within a distance of 7−7.5 Å, confirming the relatively loose character of the reverse turn.

■ CONCLUSIONS

We have proven that the Ugi reaction is a suitable approach for the macrocyclization of peptide side chains, enabling the simultaneous access to folded peptide conformations and exocyclic N-functionalization at the resulting lactam bridge. Macrocyclization efficiency was higher for side chain-to-side chain combinations based on Glu/Asp and Lys residues, while the cyclization of a carboxylic side chain with a N-terminal amine provided poorer results. Side chain-to-side chain cross-linked peptides were analyzed by NMR and MD simulation to assess the folding effect of the Ugi macrocyclization. Thus, cyclization at i → i + 3 positions led to folded structures such as a helical turn and a loose β-turn resembling a β-bulge, while the i → i + 4 combination resulted in formation of a loose α-turn. The most populated states arising from molecular dynamics simulation consist of the NMR-derived structures of the three modeled compounds, proving the preference for the folded conformations of the peptide backbone skeletons. Ongoing studies are directed to assess the effect of the N-substituent nature on the stability of specific secondary structures as well as

the utilization of such exocyclic appendages as derivatization sites, e.g., for lipidation or glycosylation.

■ EXPERIMENTAL SECTION

General. ^{1}H NMR and ^{13}C NMR spectra were recorded at 400/600 MHz for ^{1}H and 100/150 MHz for ^{13}C at 300 K. Chemical shifts (δ) are reported in parts per million relative to TMS using the residual solvent signals as secondary standards. Coupling constants (J) are reported in Hertz. Splitting patterns that could not be easily interpreted are designated as multiplet (m) or broad singlet (br. s). Carbon resonances were assigned using additional information provided by DEPT spectra recorded with phase angles of 135°. For compounds subjected to structure determination, NMR peak assignments were accomplished by analysis of standard TOCSY (mixing time 60 ms), g-COSY, g-HSQC, HMBC, and tr-ROESY (500 ms spin-lock) spectra. Peptides were characterized by electrospray ionization mass spectrometry (ESI-MS) in a hybrid quadrupole time-of-flight instrument (QTOF1) fitted with a nanospray ion source. All reagents and solvents were used as received, with the exception of CH$_2$Cl$_2$, DMF, and DIPEA that were dried by distillation from CaH$_2$ over argon prior to use as reaction solvent, and DMF was stored over 4 Å molecular sieves. Flash column chromatography was carried out using silica gel 60 (230−400 mesh), and analytical thin layer chromatography (TLC) was performed using silica gel aluminum sheets.

General Solution-Phase Peptide Synthesis. The *N*-protected amino acid (1.0 mmol, 1.0 equiv), HOBt (149 mg, 1.1 mmol, 1.1 equiv), EDC (241 mg, 1.1 mmol, 1.1 equiv), and the amino acid methyl ester (or peptide methyl ester) hydrochloride are suspended in dry CH$_2$Cl$_2$ (10 mL). Et$_3$N (0.15 mL, 1.1 mmol, 1.1 equiv) is syringed in one portion, and the resulting solution is stirred at room temperature overnight (∼12 h). The reaction mixture is then diluted with 100 mL of EtOAc, transferred to a separatory funnel and sequentially washed with 0.5 M aqueous solution of citric acid (2 × 50 mL) and a saturated aqueous suspension of NaHCO$_3$ (2 × 50 mL). The organic phase is dried over MgSO$_4$, filtered, and concentrated under reduced pressure to dryness.

General Methyl Ester Removal Procedure. The peptide (1.0 mmol) is dissolved in THF/H$_2$O (2:1, 30 mL), and LiOH (105 mg, 2.5 mmol) is added at 0 °C. The mixture is stirred at 0 °C for 3 h and then acidified with aqueous 10% NaHSO$_4$ to pH 3. The resulting phases are separated, and the aqueous phase is additionally extracted with EtOAc (2 × 50 mL). The organic phases are combined and dried over anhydrous Na$_2$SO$_4$ and concentrated under reduced pressure to yield the *C*-deprotected peptide.

General Cbz Removal Procedure. The product is dissolved in absolute EtOH (30 mL), and 10% Pd/C (80 mg) is added. The mixture is subjected successively to a hydrogen atmosphere and a vacuum and finally stirred under the hydrogen atmosphere (1 atm) for 24 h. The catalyst is removed by filtration over a pad of Celite, and the filtrate is evaporated under reduced pressure.

General Boc and tert-Butyl Ester Removal Procedure. The crude peptide is exposed to a high vacuum for 1 h before dissolving it in a 4 M HCl solution in dioxane (2 mL) for simultaneous Boc and *t*Bu removal. As the material dissolved, gas evolution could be detected and the pressure that built up inside the reaction flask is regularly relieved by opening the reaction flask. After 30 min, usually no starting material is detected by thin layer chromatography and the reaction is concentrated under a stream of dry N$_2$ for about 30 min. The volatiles are then fully removed by concentrating the resulting thick oily residue under reduced pressure in the rotary evaporator and then placing the flask under a high vacuum. If required, the hydrochloride salt can be crystallized from frozen diethyl ether.

Cbz-Leu-Lys(Boc)-Phe-Val-Glu(tBu)-Ala-OMe (1). Cbz-Glu(*t*Bu)-OH (337 mg, 1.0 mmol) was coupled to HCl·Ala-OMe (140 mg, 1.0 mmol) according to the general solution-phase peptide synthesis procedure, following by deprotection of the *N*-terminus by Cbz removal. The same protocol was employed for the coupling of Cbz-Val-OH (251 mg, 1.0 mmol) and Cbz-Phe-OH (270 mg, 0.9 mmol) to

obtain the tetrapeptide Cbz-Phe-Val-Glu(*t*Bu)-Ala-OMe with 54% yield (361 mg, 0.54 mmol) as a white amorphous solid after liquid chromatography purification in silica (*n*-hexane/AcOEt 5:1). After *N*-Cbz deprotection according to the general procedure, the tetrapeptide was coupled with Cbz-Lys(Boc)-OH (204 mg, 0.54 mmol) and Cbz-Leu-OH (125 mg, 0.47 mmol), respectively. Flash column chromatography purification (CH$_2$Cl$_2$/MeOH 25:1) furnished hexapeptide Cbz-Leu-Lys(Boc)-Phe-Val-Glu(*t*Bu)-Ala-OMe (334 mg, 0.33 mmol, 33% overall) as a white amorphous solid. ^{1}H NMR (600 MHz, DMSO-d_6): δ 8.20 (d, J = 7.6 Hz, 1H, N*H*), 8.06 (d, J = 7.2 Hz, 1H, N*H*), 7.98 (d, J = 7.8 Hz, 1H, N*H*), 7.83 (d, J = 11.1 Hz, 1H, N*H*), 7.83 (d, J = 5.3 Hz, 1H, N*H*), 7.40 (d, J = 8.3 Hz, 1H, N*H*), 7.36−7.27 (m, 5H, Ar), 7.23−7.13 (m, 5H, Ar), 6.69 (t, J = 5.4 Hz, 1H), 5.01 (s, 2H), 4.56 (m, 1H), 4.29 (dd, J = 15.2, 7.8 Hz, 1H), 4.27 (dd, J = 13.3, 8.8 Hz, 1H), 4.21−4.17 (m, 1H), 4.17 (dd, J = 8.5, 7.0 Hz, 1H), 4.01 (m, 1H), 3.61 (s, 3H), 3.00 (dd, J = 13.9, 4.6 Hz, 1H), 2.84 (dd, J = 12.1, 5.9 Hz, 2H), 2.79 (dd, J = 14.2, 9.1 Hz, 1H), 2.27−2.23 (m, 2H), 1.97−1.90 (m, 2H), 1.79−1.71 (m, 1H), 1.61−1.51 (m, 2H), 1.37 (s, 9H), 1.35 (s, 9H, C(C*H*$_3$)$_3$), 1.48−1.08 (m, 13H), 1.21 (d, J = 7.1 Hz, 3H), 0.86−0.78 (m, 12H), 0.85−0.78 (m, 1H). ^{13}C NMR (150 MHz, DMSO-d_6): δ 172.5, 172.2, 172.2, 171.5, 171.5, 170.7, 170.4, 156.0, 155.7 (CO); 137.7, 137.1 (C); 129.2, 128.5, 128.1, 127.9, 127.7, 126.3 (CH); 80.0, 77.5(C); 65.5 (CH$_2$); 57.5, 53.6, 53.2, 52.5 (CH); 52.1 (CH$_3$); 51.1, 48.0 (CH); 40.7; 39.5, 37.3, 32.0, 30.9 (CH$_2$); 30.9 (CH); 29.3 (CH$_2$); 28.4, 27.8 (CH$_3$); 26.3 (CH$_2$); 24.3(CH); 23.2 (CH$_2$); 22.6, 21.5, 19.2, 18.2, 18.1(CH$_3$). ESI-MS *m/z*: 1032.58 [M + Na]$^+$, calcd for C$_{52}$H$_{79}$O$_{13}$NaN$_7$: 1032.56. This product (334 mg, 0.33 mmol) was subjected to simultaneous Boc and *tert*-butylester removal according to the general procedure to afford peptide **1** (256 mg, 0.3 mmol, 91%). The final mixture was recrystallized from Et$_2$O/AcOEt (10 mL, 5:1) and used going forward without further purification.

General Solid-Phase Peptide Synthesis. Peptides were synthesized manually on Am-MBHA resin (250 mg, 0.45 mmol/mg) by a stepwise Fmoc/*t*Bu strategy. Amino acids were coupled using DIC/HOBt activation, and completion of the coupling reaction was monitored by the ninhydrin test. Fmoc-deprotection was carried out using 20% piperidine solution in DMF. *N*-Terminal acetylation was accomplished with 20% Ac$_2$O in DMF and DIEA for 30 min. Peptides were cleaved from the resin with the cocktail TFA/TIPS/water (95:2.5:2.5), precipitated from frozen diethyl ether, and then taken up in 1:1 acetonitrile/water and lyophilized. Linear peptides were analyzed by HPLC in a reverse-phase (RP) C18 column (4.6 × 150 mm, 5 μm) to prove purity >90%, and characterized by ESI-MS.

Ac-Val-Ile-Glu-Ala-Asn-Lys-Phe-Gly-NH$_2$ (3). The peptide (101 mg) was obtained in 94.5% purity by the general solid-phase peptide synthesis. R_t = 13.8 min. ESI-MS *m/z*: 932.54 [M + H]$^+$, calcd for C$_{43}$H$_{70}$O$_{11}$N$_{10}$: 932.52.

Ac-Phe-Lys-Gly-Pro-Ala-Asp-Ala-NH$_2$ (5). The peptide (95 mg) was obtained in 91.3% purity by the general solid-phase peptide synthesis. R_t = 10.3 min. ESI-MS *m/z*: 746.41 [M + H]$^+$, calcd for C$_{39}$H$_{59}$O$_{14}$N$_{10}$: 746.38.

Boc-Phe-Val-Ile-Glu(tBu)-OMe (7). H-Glu(*t*Bu)-OMe·HCl (254 mg, 1.0 mmol) was coupled to Cbz-Ile-OH (265 mg, 1.0 mmol) according to the general peptide coupling procedure, following by deprotection of the *N*-terminus by Cbz removal. The same protocol was employed for the coupling of Cbz-Val-OH (241 mg, 0.96 mmol). After Cbz removal, a final coupling with Boc-Phe-OH (210 mg, 0.79 mmol) was performed. Flash column chromatography purification (CH$_2$Cl$_2$/MeOH 25:1) furnished pure tetrapeptide Boc-Phe-Val-Ile-Glu(*t*Bu)-OMe (284 mg, 42% yield) as a white amorphous solid. ^{1}H NMR (400 MHz, CDCl$_3$): δ 7.29−7.07 (m, 5H), 4.71 (t, J = 6.7 Hz, 1H), 4.56−4.49 (m, 1H), 4.47 (d, J = 7.1 Hz, 1H), 4.38 (d, J = 5.6 Hz, 1H), 3.53 (s, 3H), 3.14 (dd, J = 12.3, 10.1 Hz, 1H), 2.94 (dd, J = 12.3, 4.2 Hz, 1H), 2.68−2.51 (m, 2H), 2.26−1.84 (m, 4H), 1.41 (s, 9H), 1.35 (s, 9H), 1.31−1.12 (m, 2H), 1.08−0.73 (m, 12H). ^{13}C NMR (100 MHz, CDCl$_3$): δ 173.3, 173.0, 172.2, 172.1, 171.8, 158.6 (CO); 137.3 (C); 129.4, 129.2, 127.1 (CH); 81.9, 80.5 (C); 57.5, 56.7, 55.2 (CH); 52.4 (CH$_3$); 51.7 (CH); 38.3 (CH$_2$); 35.5 (CH); 31.1 (CH$_2$); 30.4 (CH); 28.6, 28.1 (CH$_3$); 26.1, 24.8 (CH$_2$); 20.2, 19.5, 16.3, 11.6

(CH$_3$). ESI-MS (ESI-FT-ICR) m/z: 699.42 [M + Na]$^+$, calcd for C$_{35}$H$_{56}$O$_9$NaN$_4$: 699.39. This product was subjected to Boc and *tert*-butyl ester simultaneous removal according to the general procedure to afford peptide **7** (198 mg, 0.38 mmol). The final mixture was recrystallized from Et$_2$O/AcOEt (10 mL, 5:1) and used going forward without further purification.

Cbz-Val-Lys(Boc)-Leu-Phe-Ala-OMe **(9)**. H-Ala-OMe·HCl (140 mg, 1.0 mmol) was coupled to Boc-Phe-OH (265 mg, 1.0 mmol) according to the general solution-phase peptide synthesis procedure, following by deprotection of the *N*-terminus by Boc removal. The same protocol was employed for the coupling of Boc-Leu-OH (231 mg, 1.0 mmol) and Cbz-Lys(Boc)-OH (327 mg, 0.86 mmol) to obtain the tetrapeptide Cbz-Lys(Boc)-Leu-Phe-Ala-OMe. After Cbz removal, a final coupling with Cbz-Val-OH (196 mg, 0.78 mmol) was performed. Flash column chromatography purification (CH$_2$Cl$_2$/MeOH 25:1) furnished pure pentapeptide Cbz-Val-Lys(Boc)-Leu-Phe-Ala-OMe (322 mg, 39% overall) as a white amorphous solid. ^{1}H NMR (400 MHz, CDCl$_3$/CD$_3$OD 95:5): δ 7.35–7.11 (m, 10H), 5.63 (s, 2H), 4.65–4.56 (m, 1H), 4.52 (t, J = 5.7 Hz, 1H), 4.40–4.32 (m, 2H), 4.16 (q, J = 5.3 Hz, 1H), 3.65 (s, 3H), 3.25 (dd, J = 13.4, 10.8 Hz, 1H), 3.21–3.08 (m, 2H), 2.92 (dd, J = 13.3, 4.8 Hz, 1H), 2.06–1.99 (m, 1H), 1.84–1.68 (m, 2H), 1.54–1.16 (m, 7H), 1.34 (s, 9H), 1.30 (d, J = 5.2 Hz, 3H), 1.08–0.79 (m, 12H). ^{13}C NMR (100 MHz, CDCl$_3$/CD$_3$OD 95:5): δ 173.1, 172.5, 172.2, 171.1, 168.1, 158.3, 157.8 (CO); 136.5, 135.4 (C); 129.6, 129.4, 128.4, 128.3, 127.9, 127.0 (CH); 79.7 (C); 66.9 (CH$_2$); 57.6, 54.4, 53.8 (CH); 52.1(CH3); 51.4, 48.3(CH); 42.5, 40.9, 38.6, 33.2 (CH$_2$); 30.5 (CH); 29.8 (CH$_2$); 28.0 (CH$_3$); 25.3 (CH); 24.0 (CH$_2$); 20.7, 19,4, 18.2, 18.2, 17.4 (CH$_3$). ESI-MS (ESI-FT-ICR) m/z: 847.50 [M + Na]$^+$, calcd for C$_{43}$H$_{64}$O$_{10}$NaN$_6$: 847.46. This product was subjected to Boc and methyl ester removal according to the general procedures to afford peptide **9** (234 mg, 0.33 mmol). The final mixture was recrystallized from Et$_2$O/AcOEt (10 mL, 5:1) and used going forward without further purification.

General Procedure for the Ugi-Reaction-Based Macrocyclization. A solution of paraformaldehyde (0.13 mmol, 1.3 equiv), Et$_3$N (0.1 mmol, 1 equiv), and the peptide (0.1 mmol, 1 equiv) in MeOH (5 mL) was stirred for 1 h at room temperature and next diluted to 50 mL of MeOH. The isocyanide (0.2 mmol, 2 equiv) was added, and the reaction mixture was stirred for 96 h and then concentrated under reduced pressure. The crude peptide was dissolved in the minimum amount of TFA, precipitated from frozen diethyl ether, and then taken up in 1:1 acetonitrile/water and lyophilized. Peptides were purified by preparative RP-HPLC on the HPLC system LaChrom (Merck Hitachi, Germany). Separation was achieved by an RP C18 column (25 × 250 mm, 25 μm). A linear gradient from 15 to 45% of solvent B over 50 min at a flow rate of 5 mL/min was used. Detection was accomplished at 226 nm. Solvent A: 0.1% (v/v) TFA in water. Solvent B: 0.05% (v/v) TFA in acetonitrile.

N-Substituted Cyclic Peptide **2**. Peptide **1** (85 mg, 0.1 mmol), cyclohexylisocyanide (20 μL, 0.15 mmol), and paraformaldehyde (4 mg, 0.13 mmol) were reacted according to the general cyclization procedure. Purification by preparative RP-HPLC afforded the cyclic peptide **2** (55 mg, 56%) as a white amorphous solid. Purity of 98% as determined by analytical RP-HPLC. R_t = 14.96 min. ESI-MS m/z: 997.59 [M + H]$^+$, calcd for C$_{51}$H$_{74}$O$_{11}$N$_8$Na: 997.54.

N-Substituted Cyclic Peptide **4**. Peptide **3** (93 mg, 0.1 mmol), *tert*-butylisocyanide (17 μL, 0.15 mmol), and paraformaldehyde (4 mg, 0.13 mmol) were reacted according to the general cyclization procedure. Purification by preparative RP-HPLC afforded the pure cyclic peptide **4** (58 mg, 56%) as a white amorphous solid. Purity of 97% as determined by analytical RP-HPLC. R_t = 15.53 min. ESI-MS m/z: 1027.59 [M + H]$^+$, calcd for C$_{49}$H$_{79}$O$_{12}$N$_{12}$: 1027.59.

N-Substituted Cyclic Peptide **6**. Peptide **5** (89 mg, 0.1 mmol), methyl 4-isocyanobutanoate (21 μL, 0.15 mmol), and paraformaldehyde (4 mg, 0.13 mmol) were reacted according to the general cyclization procedure. Purification by preparative RP-HPLC afforded the pure cyclic peptide **6** (32 mg, 36%) as a white amorphous solid. Purity of 95% as determined by analytical RP-HPLC. R_t = 14.65 min. ESI-MS m/z: 885.44 [M + H]$^+$, calcd for C$_{41}$H$_{61}$O$_{12}$N$_{10}$: 885.45.

N-Substituted Cyclic Peptide **8**. Peptide **7** (56 mg, 0.1 mmol), *tert*-butylisocyanide (17 μL, 0.15 mmol), and paraformaldehyde (6 mg, 0.2 mmol) were reacted according to the general cyclization procedure. Purification by flash column chromatography afforded the pure cyclic peptide **8** (27 mg, 44%) as a white amorphous solid. ^{1}H NMR (600 MHz, acetone-d_6): δ 7.73 (bs, 1H), 7.51 (bs, 1H), 7.38 (bs, 1H), 7.36–6.98 (m, 6H), 5.10–5.01 (m, 1H), 4.84–4.76 (m, 1H), 4.38–4.30 (m, 1H), 4.23–4.17 (m, 1H), 3.90–3.79 (m, 2H), 3.66 (s, 3H), 3.50–3.41(m,1H), 3.15–3.05 (m, 1H), 2.63 (m, 1H), 2.54–1.88 (m, 4H), 1.70–1.60 (m, 1H), 1.34 (s, 9H), 1.41–1.14 (m, 2H), 1.04–0.81 (m, 12H). ^{13}C NMR (150 MHz, acetone-d_6): δ 176.0, 173.8, 173.1, 172.0, 171.5, 170.6 (CO); 138.9 (C); 129.7, 129.3, 127.7 (CH); 63.5, 63.2, 62.6 (CH); 53.3 (C), 51.9 (CH); 50.7 (CH$_3$); 48.0 (CH$_2$); 36.8 (CH$_2$), 36.6 (CH); 34.6 (CH$_2$); 31.5 (CH); 28.7 (CH$_3$); 25.7, 25.3 (CH$_2$), 19.9, 19.8, 16.1, 12.3 (CH$_3$). ESI-MS (ESI-FT-ICR) m/z: 638.36 [M + Na]$^+$, calcd for C$_{32}$H$_{49}$O$_7$NaN$_5$: 638.35.

N-Substituted Cyclic Peptide **10**. Peptide **9** (71 mg, 0.1 mmol), cyclohexylisocyanide (20 μL, 0.15 mmol), and paraformaldehyde (6 mg, 0.2 mmol) were reacted according to the general cyclization procedure. Purification by flash column chromatography afforded the pure cyclic peptide **10** (42 mg, 51%) as a white amorphous solid. ^{1}H NMR (600 MHz, CDCl$_3$/CD$_3$OD 95:5): δ 7.51–7.29 (m, 10H), 5.26 (d, J = 12.4 Hz, 1H), 5.22 (d, J = 12.4 Hz, 1H), 4.77 (dd, J = 10.2, 3.7 Hz, 1H), 4.69 (dd, J = 9.5, 3.1 Hz, 1H), 4.47 (d, J = 6.0 Hz, 1H), 4.35 (m, 1H), 4.21 (q, J = 5.7 Hz, 1H), 4.12 (d, J = 16.0 Hz, 1H), 3.97 (d, J = 16.0 Hz, 1H), 3.84–3.77 (m, 1H), 3.59–3.50 (m, 1H), 3.33–3.23 (m, 1H), 3.07 (dd, J = 14.3, 10.4 Hz, 1H), 2.08–2.00 (m, 1H), 1.98–1.90 (m, 2H), 1.89–1.69 (m, 7H), 1.69–1.24 (m, 10H), 1.52 (d, J = 7.2 Hz, 3H), 1.12 (d, J = 6.7 Hz, 3H), 1.08 (d, J = 6.4 Hz, 6H), 1.05 (d, J = 6.5 Hz, 3H). ^{13}C NMR (150 MHz, CDCl$_3$/CD$_3$OD 95:5): δ 173.1, 172.8, 171.6, 171.4, 171.1, 168.3, 156.8 (CO); 136.6, 135.9 (C); 128.3, 127.9, 127.9, 127.5, 127.1, 126.2 (CH), 66.3 (CH$_2$); 57.5, 55.1, 53.5, 50.9, 49.3 (CH); 49.2 (CH$_2$), 48.9 (CH); 48.3, 40.3, 36.4, 32.0, 31.9 (CH$_2$); 30.9 (CH); 27.4, 26.4 (CH$_2$), 24.9 (CH), 24.4, 24.1 (CH$_2$), 21.9, 20.7, 18.4, 17.2, 16.2 (CH$_3$). ESI-MS (ESI-FT-ICR) m/z: 854.48 [M + Na]$^+$, calcd for C$_{45}$H$_{65}$O$_8$NaN$_7$: 854.48.

NMR Structure Determination. Cross-peaks in t-ROESY spectra were assigned and integrated in *Sparky NMR*.[26] Distance constraints from ROE intensities were generated using pseudoatom corrections where needed and placed into three groups: strong (2.8 Å upper limit), medium (3.5 Å upper limit), and weak (5.0 Å upper limit). The lower limit for NOE restraints was always maintained at 1.8 Å. Backbone dihedral angle restraints were inferred from $^3J_{NHCHa}$ coupling constants in the 1D spectrum at 300 K, and φ was restrained to −120 ± 30° for $^3J_{NHCHa}$ ≥ 8 Hz as reported by Fairlie et al.[8e] Peptide bond ω angles were all set *trans*. Structure calculations were carried out using the *Xplor-NIH 2.33* package.[24] The calculations were performed using the standard force field parameter set (PARALLHDG.PRO) and topology file (TOPALLHDG.PRO) within *Xplor-NIH* with in-house modifications to ensure peptide cyclization and amide *N*-substitution. Structures were visualized and analyzed using *VMD-Xplor*.

NMR structure determination was performed through simulated annealing regularization and refinement in torsion angle space, using experimental data as interproton distances and dihedral angles restraints. For simulated annealing regularization, 200 starting structures were randomly generated. A 100 ps molecular dynamics simulation at 3500 K was performed with a time step of 3 fs. The system was cooled from 3500 to 25 K, with a temperature step of 12.5 K. At each temperature step, 0.2 ps of molecular dynamics simulation was performed. A 500-step torsion angle minimization was performed, and finally, the system was optimized by means of 500-step conjugated gradient Powell Cartesian minimization.

The refinement protocol consisted of a slow cooling simulated annealing from the regularized structures. A 10 ps molecular dynamics simulation at 3000 K was achieved with a time step of 3 fs. The system was cooled with a temperature step of 12.5 K and a simulation time of 0.2 ps at each temperature. A 500 torsion angle minimization was performed; afterward, a second 500-step minimization was achieved in Cartesian coordinates. A final 1000-step Powell minimization with an

energy function nondependent of experimental restraints was executed. (For more details, see the Supporting Information.)

Molecular Dynamics Simulations. Molecular dynamics simulation was performed with the NAMD[27] software taking as starting coordinates the corresponding NMR structure. The CHARMM-36[28] force field was used with convenient parametrizations for nonstandard residues, i.e., peptide N-funcionalized cyclization, with the help of the Paratool plugin within the VMD[29] molecular package. Before each simulation, a 60 ps MD equilibration was performed. All simulations were performed using periodic boundary conditions in a cubic box with explicit solvent. The model proposed by Laaksonen[30] was employed for the treatment of DMSO molecules. The simulation temperature was always set to 310 K, using Langevin dynamics for temperature control (damping coefficient of 1/ps). A Langevin piston was utilized for maintaining a pressure of 1 atm. A 12 Å cutoff with a switching function was employed for nonbonded van der Waals and electrostatics interactions. A 2 fs time step was always used with the SHAKE algorithm for freeze hydrogen−heavy atom interatomic distances. Final trajectories were analyzed and visualized in VMD[29] and Vega ZZ[31] softwares.

■ ASSOCIATED CONTENT

Ⓢ Supporting Information

ESI-MS and HPLC chromatograms of linear peptides produced by solid-phase peptide synthesis. HPLC chromatograms, ESI-MS, and NMR spectra of all final cyclic peptides. The Supporting Information is available free of charge on the ACS Publications website at DOI: 10.1021/acs.joc.5b00858.

■ AUTHOR INFORMATION

Corresponding Authors
*E-mail: wessjohann@ipb-halle.de.
*E-mail: dgr@fq.uh.cu.

Notes

The authors declare no competing financial interest.

■ REFERENCES

(1) (a) Robinson, J. A. J. Pept. Sci. 2013, 19, 127. (b) Craik, D. J.; Fairlie, D. P.; Liras, S.; Price, D. Chem. Biol. Drug Des. 2013, 81, 136. (c) Liskamp, R. M. J.; Rijkers, D. T. S.; Kruijtzer, J. A. W.; Kemmink, J. ChemBioChem 2011, 12, 1626. (d) Adessi, C.; Soto, C. Curr. Med. Chem. 2002, 9, 963.

(2) (a) White, C. J.; Yudin, A. K. Nat. Chem. 2011, 3, 509. (b) Marsault, E.; Peterson, M. L. J. Med. Chem. 2011, 54, 1961. (c) Hruby, V. J. Nat. Rev. Drug Discovery 2002, 1, 847.

(3) (a) Hill, T. A.; Shepherd, N. E.; Diness, F.; Fairlie, D. P. Angew. Chem., Int. Ed. 2014, 53, 13020. (b) Robinson, J. A. Acc. Chem. Res. 2008, 41, 1278. (c) Garner, J.; Harding, M. M. Org. Biomol. Chem. 2007, 5, 3577. (d) Renner, C.; Moroder, L. ChemBioChem 2006, 7, 868. (e) Woolley, G. A. Acc. Chem. Res. 2005, 38, 486. (f) Loughlin, W. A.; Tyndall, J. D. A.; Glenn, M. P.; Fairlie, D. P. Chem. Rev. 2004, 104, 6085.

(4) (a) Rivera, D. G.; Vasco, A. V.; Echemendía, R.; Concepción, O.; Pérez, C. S.; Gavín, J. A.; Wessjohann, L. A. Chem.—Eur. J. 2014, 20, 13150. (b) Gokhale, A.; Weldeghiorghis, T. K.; Taneja, V.; Satyanarayanajois, S. D. J. Med. Chem. 2011, 54, 5307. (c) Bodé, C. A.; Bechet, T.; Prodhomme, E.; Gheysen, K.; Gregoir, P.; Martins, J. C.; Muller, C. P.; Madder, A. Org. Biomol. Chem. 2009, 7, 3391. (d) Singh, Y.; Dolphin, G. T.; Razkin, J.; Dumy, P. ChemBioChem 2006, 7, 1298. (e) Hruby, V. J. Nat. Rev. 2002, 1, 847. (f) Tuchscherer, G.; Grell, D.; Mathieu, M.; Mutter, M. J. Pept. Res. 1999, 54, 185.

(5) Hruby, V. J.; al-Obeidi, F.; Kazmierski, W. Biochem. J. 1990, 268, 249.

(6) (a) Giordanetto, F.; Kihlberg, J. J. Med. Chem. 2014, 57, 278. (b) Driggers, E. M.; Hale, S. P.; Lee, J.; Terrett, N. K. Nat. Rev. Drug Discovery 2008, 7, 608.

(7) (a) Sieber, S. A.; Marahiel, M. A. Chem. Rev. 2005, 105, 715. (b) Kohli, R. M.; Walsh, C. T. Chem. Commun. 2003, 3, 297.

(8) (a) de Araujo, A. D.; Hoang, H. N.; Kok, W. M.; Gupta, P.; Hill, T. A.; Driver, R. W.; Price, D. A.; Liras, S.; Fairlie, D. P. Angew. Chem., Int. Ed. 2014, 53, 6965. (b) Shepherd, N. E.; Hoang, H. N.; Abbenante, G.; Fairlie, D. P. J. Am. Chem. Soc. 2009, 131, 15877. (c) Mills, N. L.; Daugherty, M. D.; Franke, A. D.; Guy, K. J. Am. Chem. Soc. 2006, 128, 3496. (d) Woolley, G. A.; Jaikaran, A. S. I.; Berezovski, M.; Calarco, J. P.; Krylov, S. N.; Smart, O. S.; Kumita, J. R. Biochemistry 2006, 45, 6075. (e) Shepherd, N. E.; Hoang, H. N.; Abbenante, G.; Fairlie, D. P. J. Am. Chem. Soc. 2005, 127, 2974. (f) Taylor, J. W. Biopolymers 2002, 66, 49. (g) Condon, S. M.; Morize, I.; Darnbrough, S.; Burns, C. J.; Miller, B. E.; Uhl, J.; Burke, K.; Jariwala, N.; Locke, K.; Krolikowski, P. H.; Kumar, N. V.; Labaudiniere, R. F. J. Am. Chem. Soc. 2000, 122, 3007.

(9) (a) Holland-Nell, K.; Meldal, M. Angew. Chem., Int. Ed. 2011, 50, 5204. (b) Jacobsen, Ø.; Maekawa, H.; Ge, N.-H.; Görbitz, C. H.; Rongved, P.; Ottersen, O. P.; Amiry-Moghaddam, M.; Klaveness, J. J. Org. Chem. 2011, 76, 1228. (c) Cantel, S.; Isaad, A. L. C.; Scrima, M.; Levy, J. J.; DiMarchi, R. D.; Rovero, P.; Halperin, J. A.; D'Ursi, A. M.; Papini, A. M.; Chorev, M. J. Org. Chem. 2008, 73, 5663.

(10) (a) Hilinski, G. J.; Kim, Y.-W.; Hong, J.; Kutchukian, P. S.; Crenshaw, C. M.; Berkovitch, S. S.; Chang, A.; Ham, S.; Verdine, G. L. J. Am. Chem. Soc. 2014, 136, 12314. (b) Kim, Y.-W.; Kutchukian, P. S.; Verdine, G. L. Org. Lett. 2010, 12, 3046. (c) Kutchukian, P. S.; Yang, J. S.; Verdine, G. L.; Shakhnovich, E. I. J. Am. Chem. Soc. 2009, 131, 4622. (d) Walensky, L. D.; Kung, A. L.; Escher, I.; Malia, T. J.; Barbuto, S.; Wright, R. D.; Wagner, G.; Verdine, G. L.; Korsmeyer, S. J. Science 2004, 305, 1466. (e) Blackwell, H. E.; Sadowsky, J. D.; Howard, R. J.; Sampson, J. N.; Chao, J. A.; Steinmetz, W. E.; O'Leary, D. J.; Grubbs, R. H. J. Org. Chem. 2001, 66, 5291. (f) Schafmeister, C. E.; Po, J.; Verdine, G. L. J. Am. Chem. Soc. 2000, 122, 5891. (g) Blackwell, H. E.; Grubbs, R. H. Angew. Chem., Int. Ed. 1998, 37, 3281.

(11) (a) Cristau, P.; Temal-Laïb, T.; Bois-Choussy, M.; Martin, M.-T.; Vors, J.-P.; Zhu, J. Chem.—Eur. J. 2005, 11, 2668. (b) Bondebjerg, J.; Grunnet, M.; Jespersen, T.; Meldal, M. ChemBioChem 2003, 4, 186. (c) Reid, R. C.; Kelso, M. J.; Scanlon, M. J.; Fairlie, D. P. J. Am. Chem. Soc. 2002, 124, 5673.

(12) (a) Meyer, F.-M.; Collins, J. C.; Borin, B.; Bradow, J.; Liras, S.; Limberakis, C.; Mathiowetz, A. M.; Philippe, L.; Price, D.; Song, K.; James, K. J. Org. Chem. 2012, 77, 3099. (b) Feliu, L.; Planas, M. Int. J. Pept. Res. Ther. 2005, 11, 53—97.

(13) (a) Masson, G.; Neuville, L.; Bughin, C.; Fayol, A.; Zhu, J. Top. Heterocycl. Chem. 2010, 25, 1. (b) Wessjohann, L. A.; Rivera, D. G.; Vercillo, O. E. Chem. Rev. 2009, 109, 796.

(14) (a) Rotstein, B. H.; Zaretsky, S.; Rai, V.; Yudin, A. K. Chem. Rev. 2014, 114, 8323. (b) Koopmanschap, G.; Ruijter, E.; Orru, R. V. A. Beilstein J. Org. Chem. 2014, 10, 544. (c) Wessjohann, L. A.; Rhoden, C. R. B.; Rivera, D. G.; Vercillo, O. E. Top. Heterocycl. Chem. 2010, 23, 199.

(15) Failli, A.; Immer, H.; Götz, M. D. Can. J. Chem. 1979, 57, 3257.

(16) (a) Rivera, D. G.; Wessjohann, L. A. J. Am. Chem. Soc. 2009, 131, 3721. (b) Rivera, D. G.; Vercillo, O. E.; Wessjohann, L. A. Org. Biomol. Chem. 2008, 6, 1787. (c) Rivera, D. G.; Wessjohann, L. A. J. Am. Chem. Soc. 2006, 128, 7122. (d) Wessjohann, L. A.; Rivera, D. G.; Coll, F. J. Org. Chem. 2006, 71, 7521. (e) Wessjohann, L. A.; Voigt, F.; Rivera, D. G. Angew. Chem., Int. Ed. 2005, 44, 4785.

(17) (a) Barreto, A. F. S.; Vercillo, O. E.; Birkett, M. A.; Caulfield, J. C.; Wessjohann, L. A.; Andrade, C. K. Z. Org. Biomol. Chem. 2011, 9, 5024. (b) Vercillo, O. E.; Andrade, C. K. Z.; Wessjohann, L. A. Org. Lett. 2008, 10, 205.

(18) Ricardo, M. G.; Morales, F. E.; Garay, H.; Reyes, O.; Vasilev, D.; Wessjohann, L. A.; Rivera, D. G. Org. Biomol. Chem. 2015, 13, 438.

(19) Hili, R.; Rai, V.; Yudin, A. K. J. Am. Chem. Soc. 2010, 132, 2889.

(20) (a) White, C. J.; Hickey, J. L.; Scully, C. C. G.; Yudin, A. K. J. Am. Chem. Soc. 2014, 136, 3728. (b) Zaretsky, S.; Scully, C. C. G.; Lough, A. J.; Yudin, A. K. Chem.—Eur. J. 2013, 19, 17668. (c) Scully,

C. C. G.; Rai, V.; Poda, G.; Zaretsky, S.; Burns, D. C.; Houliston, R. S.; Lou, T.; Yudin, A. K. *Chem.—Eur. J.* **2012**, *18*, 15612.

(21) (a) Chatterjee, J.; Chaim, G.; Hoffman, A.; Kessler, H. *Acc. Chem. Res.* **2008**, *41*, 1331. (b) Chatterjee, J.; Ovadia, O.; Zahn, G.; Marinelli, L.; Hoffman, A.; Gilon, C.; Kessler, H. *J. Med. Chem.* **2007**, *50*, 5878. (c) Wessjohann, L. A.; Andrade, C. K. Z.; Vercillo, O. E.; Rivera, D. G. *Targets Heterocycl. Syst.* **2006**, *10*, 24.

(22) Sewald, N.; Jakubke, H.-D. *Peptides: Chemistry and Biology*; Wiley-VCH: Weinheim, 2002.

(23) (a) Estieu-Gionnet, K.; Guichard, G. *Expert Opin. Drug Discovery* **2011**, *6*, 937. (b) Henchey, L. K.; Jochim, A. L.; Arora, P. S. *Curr. Opin. Chem. Biol.* **2008**, *12*, 692. (c) Garner, J.; Harding, M. M. *Org. Biomol. Chem.* **2007**, *5*, 3577.

(24) (a) Schwieters, C. D.; Kuszewski, J. J.; Clore, G. M. *Prog. NMR Spectrosc.* **2006**, *48*, 47. (b) Schwieters, C. D.; Kuszewski, J. J.; Tjandra, N.; Clore, G. M. *J. Magn. Reson.* **2003**, *160*, 66.

(25) Chan, A. W. E.; Hutchinson, E. G.; Harris, D.; Thornton, J. M. *Protein Sci.* **1993**, *2*, 1574.

(26) Goddard, T. D.; Kneller, D. G. *SPARKY 3*; University of California, San Francisco: San Francisco, CA.

(27) Phillips, J. C.; Braun, R.; Wang, W.; Gumbart, J.; Tajkhorshid, E.; Villa, E.; Chipot, C.; Skeel, R. D.; Kale, L.; Schulten, K. *J. Comput. Chem.* **2005**, *26*, 1781.

(28) MacKerell, A. D.; Feig, M.; Brooks, C. L. *J. Am. Chem. Soc.* **2004**, *126*, 698.

(29) Humphrey, W.; Dalke, A.; Schulten, K. *J. Mol. Graphics* **1996**, *14*, 33.

(30) Laaksonen, A. *J. Phys. Chem. A* **2001**, *105*, 1702.

(31) Pedretti, A.; Villa, L.; Vistoli, G. *J. Mol. Graphics* **2002**, *21*, 47.